

# Physical, Chemical and Mechanical Characterization of Polypropylene Biocomposites with Fibers from *Euterpe precatoria*, *Paullinia cupana* var. *sorbilis* (mart.) *ducke* and *Astrocaryum aculeatum*

## *Caracterização Física, Química e Mecânica de Biocompósitos de Polipropileno com Fibras de Euterpe precatoria, Paullinia cupana* var. *sorbilis* (Mart.) *ducke* e *Astrocaryum aculeatum*

Dorian L. Oliveira,<sup>a</sup> Wamber B. Souza,<sup>b,\*</sup> Roberta L. S. Bernardino,<sup>c</sup> Genilson P. Santana,<sup>d</sup> Flávio A. Freitas,<sup>e</sup> Antonio C. Kieling,<sup>f</sup> Sérgio Duvoisin Junior,<sup>f</sup> Cledson R. Souza,<sup>g</sup> Silma S. Barros<sup>h</sup>

The growing concern over the improper disposal of Amazonian fruit residues and the increasing demand for sustainable materials motivated this study. This work aimed to develop biocomposites from açai, guaraná, and tucumã residues incorporated into a polypropylene (PP) matrix *via* injection molding. The materials were produced and characterized by lignocellulosic analysis, X-ray diffraction (XRD), and scanning electron microscopy (SEM). The fibers presented moisture content  $\leq 22.4\%$ , cellulose  $\leq 50.9\%$ , hemicellulose  $\leq 37.8\%$ , lignin  $\leq 45.7\%$ , and crystallinity  $\leq 28.4\%$ . Thermal behavior, analyzed by thermogravimetric analysis (TGA) and differential scanning calorimetry (DSC), revealed transformation ranges of 167.8–464.0 °C for the biocomposites and 437.3 °C for neat PP, with degradation onset at 300 and 396.8 °C, respectively. Although the biocomposites exhibited lower tensile strength than neat PP, mechanical testing (tensile and flexural) indicated distinct rupture patterns and phase separation. These findings support the potential of Amazonian fruit residues as reinforcing agents in sustainable polymeric materials with industrial applicability.

**Keywords:** Amazonian fibers; açai; tucumã; guarana; composite.

## 1. Introduction

The Amazon region probably has the greatest diversity of native and exotic fruit species.<sup>1</sup> However, an area of approximately 9,000 km<sup>2</sup> of the Brazilian Amazon has been reduced due to deforestation,<sup>2</sup> which implies the loss of a part of this biodiversity. On the other hand, plant extractivism has become widespread as a great Brazilian environmental solution for containing deforestation in the Amazon.<sup>3</sup> Despite this, in the case of plant extractivism, as well as in the food, pharmaceutical and cosmetic industries, there is a significant production of waste, especially fibrous waste and cakes. In the case of exploitation for commercialization and industrialization of the Amazonian fruits of *Euterpe precatoria* (açai), *Paullinia cupana* (guaraná) and *Astrocaryum aculeatum* (tucumã), these types of waste are also generated, although they do have high potential for reuse.

The fruit of açai is globose, with a black-purple coloration when ripe and is formed by three layers: the exocarp, with a smooth surface; the mesocarp, characterized by the edible pulp, surrounded by mesocarpic fibers, in addition to the endocarp, located below the mesocarpic fibers.<sup>4</sup>

The commercial exploitation of açai fruits is similar to that of the fruits of the palm trees *Euterpe edulis* and *oleracea*,<sup>5</sup> which are also present in the region. The extraction of the fruit pulp of açai has increased its value in local, regional, national markets<sup>6</sup> and, in the last decade, in the international market, thus contributing to the increase in exports.<sup>7</sup> This pulp is used in the preparation of food and beverages.<sup>8</sup>

The main residue from the industrial processing of açai is the fiber-rich core that corresponds to approximately 85% of the fruit. However, there is no adequate disposal for the tons of this fibrous residue, so it is usually disposed of indiscriminately in the environment.<sup>7</sup> Based on the 2021 harvest, the states of Pará (PA) and Amazonas (AM) stand out as the largest Brazilian producers of açai in terms of permanent crops.<sup>9</sup> Consequently, a total of 1,179,286.60 tons year<sup>-1</sup> of fibrous residues was generated in PA and 70,343.45 tons year<sup>-1</sup> in AM. In the capitals, Belém (PA) 612 tons year<sup>-1</sup> and Manaus (AM) 479.4 tons year<sup>-1</sup>.

<sup>a</sup>Instituto Federal de Educação, Ciência e Tecnologia do Amazonas, Zip Code 69020-120, Manaus-AM, Brazil

<sup>b</sup>Universidade Federal do Amazonas, Colegiado de Zootecnia, Zip Code 69152-240, Parintins-AM, Brazil

<sup>c</sup>Universidade Federal do Amazonas, Programa de Pós-Graduação em Física, Zip Code 69067-005, Manaus-AM, Brazil

<sup>d</sup>Universidade Federal do Amazonas, Departamento de Química, Zip Code 69067-005, Manaus-AM, Brazil

<sup>e</sup>Centro de Biotecnologia da Amazônia, Zip Code 69075-351, Manaus-AM, Brazil

<sup>f</sup>Universidade do Estado do Amazonas, Escola Superior de Tecnologia, Zip Code 69050-020, Manaus-AM, Brazil

<sup>g</sup>Instituto Federal de Educação, Ciência e Tecnologia do Amazonas, Departamento de Engenharia Mecânica, Zip Code 69020-120, Manaus-AM, Brazil

<sup>h</sup>Universidade de São Paulo, Escola de Engenharia de Lorena, Departamento de Engenharia de Materiais, Zip Code 12602-810, São Paulo-SP, Brazil

\*E-mail: [wambersa@ufam.edu.br](mailto:wambersa@ufam.edu.br)

Submissão: 2 de Abril de 2025

Aceite: 21 de Outubro de 2025

Publicado online: 13 de Novembro de 2025

The tucumã fruit is globose to ellipsoid, with a smooth and yellowish epicarp, a fleshy and orange mesocarp and a hard and black endocarp.<sup>10</sup> According to Kieling,<sup>11</sup> the pulp is part of the daily life of the population of the state of Amazonas and is consumed fresh in various dishes, such as sandwiches, tapiocas, creams and ice cream.

The fruit of the species guaraná has an ellipsoid/globose shape and its seed has an ovoid shape<sup>12</sup> can be used to produce extracts for soft drinks and energy drinks for the beverage industry and inputs for the pharmaceutical industry,<sup>13</sup> however, it also generates considerable amounts of fibrous waste. Data from the literature show that about 92 tons year<sup>-1</sup> of fibrous residues of guaraná alone<sup>14</sup> and 49.8 tons year<sup>-1</sup> of tucumã are discarded.<sup>11</sup> Thus, there is an urgent need to develop technologies that enable the reuse of these fibrous residues that currently have no appropriate destination. In this case, the use of these fibrous residues could be a viable alternative for reinforcing polymer matrices in the form of composites. For example, lignocellulosic fibers are of interest to the automobile and aviation industry mainly because they are environmentally friendly, have a low cost and have superior mechanical properties.<sup>15</sup> However, beforehand, it is necessary to determine the crystal structure and the physicochemical properties of these lignocellulosic fibers. Among the physicochemical properties are the different proportions of cellulose, hemicellulose and lignin,<sup>16</sup> as well as moisture.<sup>17</sup>

Thus, plant fibers are the most common types of fibers that reinforce biocomposites produced with polymer matrices. They act directly on the mechanical properties and improve the strength and mechanical performance of polymer biocomposites. Numerous researchers have explored various types of natural fibers, including coir, hemp, banana, borassus, sisal, jute, tamarind, flax, kapok, and kenaf, among others, as potential reinforcements in polymer composites.<sup>18,19</sup> While natural fibers offer certain advantages as previously mentioned, they also present several challenges when used in polymer matrix composites.<sup>20</sup> These drawbacks include their hydrophilic nature, high moisture absorption, poor resistance to elevated temperatures, inconsistency in fiber properties, and weak bonding with hydrophobic polymeric matrices. Among various natural materials, natural fibers present several advantages over synthetic materials when used as reinforcements in composites. These advantages stem from their renewable characteristics and eco-friendly nature, making them suitable for a wide range of applications. Furthermore, the production process of polymer biocomposites using natural fibers can be easily implemented through conventional plastic production techniques, such as extrusion and injection molding of polypropylene (PP) polymer matrices.<sup>21</sup> This ease of manufacturing adds to the appeal of natural fiber-reinforced composites in industrial applications.<sup>22</sup> This study develops and characterizes innovative biocomposites utilizing residues from Amazonian fruits (açai, tucumã, and guaraná) combined with polypropylene (PP) through plastic

injection molding. The research comprehensively evaluates the physical, chemical, and thermal properties of these biocomposites, as well as their mechanical performance. Additionally, it assesses their potential as a sustainable solution for fruit waste management and explores possible applications in various industries.

## 2. Experimental

### 2.1. Açai, guaraná and tucumã residues: materials and preparation of samples

The development of this work was carried out using lignocellulosic fibers from fruit residues of açai and endocarps of tucumã obtained from local traders in Manaus (Amazonas, Brazil); and roasted seeds of guaraná fruits from the production of soft drink extracts donated by a factory in the industrial district of Manaus. The polypropylene grade H 301 (Braskem), characterized by a medium melt flow index and formulated with additives for general-purpose applications, with an average particle size of 3,500 µm, was supplied by a plastic injection molding company located in the industrial district of Manaus.

To conduct this study, the endocarps of açai were disinfected with a bleach solution (2.5% NaClO) in 1 L of drinking water for 10 min<sup>23,24</sup> and then dried in the sun for 8 h. Subsequently, 20-mesh fibers were obtained with the use of manual defibration and grinding in a knife mill (SP Labor) for the larger fibers present in the endocarps. The tucumã endocarps were disinfected, dried, then broken with the aid of a sledgehammer, whereby the endosperms were separated, and the endocarp was subjected to grinding in a similar way to the previous procedure. The residues of processed seeds of guaraná, which were already dry after torrefaction, were sieved in a 20-mesh sieve.

### 2.2. Biocomposites: materials and preparation of the samples

A Haitian Hayuan (MA1600, Chine) injection molding machine is used to manufacture the samples. The biocomposites were produced with particles previously dried in an oven (~60 °C) for 6 hours and cooled inside it, and then placed in boxes with lids to prevent moisture absorption. Each manufacturing batch considers 2 kg of materials. The particles are weighted on a precision scale (Prix 3400 with a resolution of 0.001 g) and hand-mixed for 5 minutes to ensure homogeneity of the samples. Preliminary tests were conducted to set the injection machine to provide acceptable surface finish and adequate sample reproducibility. The temperature of the four positions along the injection tube was adjusted to 195 °C, with an injection pressure of 80 bar. The dimension of the injected WPC plates is 178×118×3.2 mm<sup>3</sup>. The proportions of PP and dry fibers ≤ 20 mesh of açai (A), guaraná (G) and tucumã

(T): PP:100 (named PP); PP:A ratio of 90:10 (named PP:A) (Figure 1); PP:G ratio of 90:10 (named PP:G); PP:T ratio of 90:10 (named PP:T); PP:A:G ratio of 90:5:5 (named PP:A:G); PP:A:T ratio of 90:5:5 (named PP:A:T); PP:G:T ratio of 90:5:5 (named PP:G:T); and PP:A:G:T ratio of 90:3.4:3.3:3.3 (named PP:A:G:T), which correspond to the percentages in masses for 1 kg of materials. The proportions produced were injected as described by da Silva Junior *et al.*<sup>13</sup>

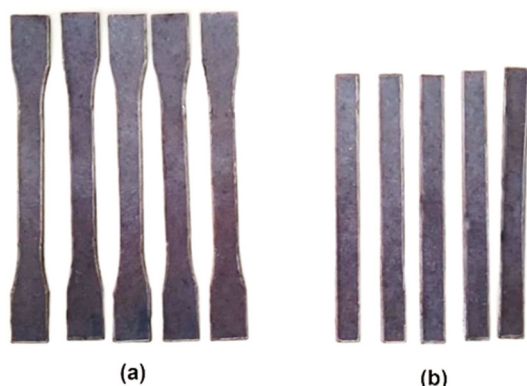


**Figure 1.** Test specimens for mechanical tests with the composite of PP and açai fibers (PP:A:90:10 (PP:A)): (a) tensile and (b) flexural

### 2.3. Lignocellulosic analysis

The lignocellulosic analysis of açai, tucumã and guaraná was performed to determine the moisture, amount of cellulose, hemicellulose and lignin. The analyses were performed according to the recommendation of the Brazilian Agricultural Research Company.<sup>25</sup> Thus, the determination of extractives of the samples was performed with ethyl alcohol 70%. The amount of cellulose, lignin and hemicellulose was obtained with the following reagents: sodium chlorite (NaClO<sub>2</sub>, 80%, Dinâmica); acetic acid (CH<sub>3</sub>COOH, ≥ 99.85%, Sigma Aldrich); aqueous solution of sodium hydroxide (NaOH, 17.5% distilled water, Vetec); and an aqueous solution of sulfuric acid (H<sub>2</sub>SO<sub>4</sub>, 72% (m/m), Biotec). The extractives and moisture analyses were performed in triplicate and the rest were in duplicate.

#### 2.3.1. X-ray diffraction (XRD)

To determine the crystallinity of fibers from açai, tucumã, and guaraná, 20-mesh fiber samples were analyzed using an X-ray diffractometer (XRD-7000-maxima/Shimadzu), with a copper anode as the source of X-ray radiation (Cu Kα = 0.15406 nm), with a voltage of 40 kV and 30 mA of current, and scanning ranging from 10° to 80° (2θ) at the speed of 2° min<sup>-1</sup> and 0.02° pitch. The crystallinity was calculated using the Ruland method and equation (1).<sup>26</sup>

$$C (\%) = \frac{I_p}{(I_p + I_a)} \quad (1)$$

where: C (%) = percentage of crystalline phase;

$I_p$  = integration of the peak area assigned to the crystalline phase;  $I_a$  = integration of the amorphous region.

#### 2.3.2. Optical microscopy (OM)

The granulometry of the PP and of the fibers of açai, tucumã and guaraná was determined using the software Image J 1.54 (open source) and images were obtained using a Kowa stereoscope and Coleman optical microscope (N107) with a camera (Omron Sentech, STC C83USB).

#### 2.3.3. Scanning electron microscopy (SEM)

Scanning electron microscopy (Jeol: JSM-IT500HR) of the fibers and the biocomposites was performed with high resolution images magnified with working distance of 10.4 mm and acceleration voltage of 5 kV. The samples were fixed on a double-sided carbon tape attached to a metal stub and vacuum metallized for 4 min in a metallizer (Jeol, DII-29010sctr Smart Coater). With the aid of a secondary electron detector coupled to the scanning electron microscope, the micrographs were obtained.

#### 2.3.4. Thermal analysis: thermogravimetric analysis (TGA) and differential scanning calorimetry (DSC)

TGA was performed on samples of fibers and biocomposites of approximately 10 mg in a platinum crucible. Measurements were taken in a nitrogen atmosphere (50 mL min<sup>-1</sup>), with a mass variation as a function of a temperature range of 25 to 600 °C and heating ramp of 10 °C min<sup>-1</sup> in a thermogravimetric analyzer (Shimadzu TGA-50H). The DSC measurements were performed with 5 mg samples in a differential scanning calorimeter (Shimadzu, DSC-60) with a nitrogen atmosphere and a gas flow of 50 mL min<sup>-1</sup>. Temperature variations were between 25 °C and 500 °C with a rate of 10 °C min<sup>-1</sup>.

#### 2.3.5. Fourier-transform infrared spectroscopy (FTIR)

The FTIR spectra of the fiber, PP, and biocomposite samples were obtained in the wavelength region of 500 to 4000 cm<sup>-1</sup> using a spectrometer (Shimadzu, IRAffinity-1s, 70 scans/IRTracer-100, 45 scans) with a resolution of 4 cm<sup>-1</sup> in transmittance mode. The solid samples were pressed in KBr and analyzed with 128 scans, 4 cm<sup>-1</sup> resolution, and a mirror velocity of 0.05 cm s<sup>-1</sup>.

#### 2.3.6. Mechanical tests: tension and flexion

Three-point tensile and bending mechanical tests for PP and bioproduct samples were carried out in accordance with ASTM D638-14 and ASTM D790-03, respectively. From the flat plates obtained from plastic injection, the specimens were outlined in Corel Draw Laser and cut on a Router Laser machine (VS6040).

For the tensile test, type I specimens were manufactured, made of reinforced composites, in the form of dumbbells. For the flexion test, test specimens were made from molding materials (thermoplastic) in accordance with item 7.4 of the standard. Each sample was tested in quintuplicates on an

Instron 5984 testing machine with a load of 150 kN, a speed of 10 mm min<sup>-1</sup> and an ambient temperature of 23 ± 2 °C.

The results selected in the test were resistance and modulus of elasticity in tension and flexion.

### 3. Results and Discussion

#### 3.1. Physical, chemical and thermal characteristics of the lignocellulosic fibers

The results show the following moisture contents for the fibers studied in their natural state and which had an average size of ≤ 20 mesh: i) tucumã: 12.89% (± 0.05); ii) guaraná: 10.73% (± 0.27); and iii) açai: 22.35% (± 0.06). There is little data on the moisture of these fibers in their natural state, and reported data basically show some levels of moisture content under certain drying conditions. Oliveira Júnior *et al.*<sup>27</sup> cite moisture levels of 10.65% after 3 h of drying at 105 °C for guaraná fiber (≤ 20 mesh), which is very close to the moisture levels found in our study. For açai fiber, the literature mentions that the moisture level is 7.17% when dried for 3 h at 65 °C using ≤ 40 mesh fibers.<sup>28</sup> Another important characteristic in the results obtained is that the fiber of guaraná has a moisture level that is very close to that of tucumã.

In terms of the production of biocomposites with these fibers, it is noted that heating for 30 minutes at 105 °C followed by desiccation for 20 minutes is a recommended procedure for the use of these fibers in the process of injection or extrusion with polymer matrices. According to Yan *et al.*<sup>29</sup> hemicellulose is directly responsible for the moisture content in plant fibers. In fact, Figure 2a shows the proximity in hemicellulose content of guaraná and tucumã fibers. The results also reveal that cellulose and lignin in the fibers of tucumã are higher than in those of açai and guaraná, which is similar to the results of Kieling *et al.*<sup>13</sup> These authors found 49.4 ± 0.9% and 37.4 ± 1.3% respectively for cellulose and lignin contents. Guaraná fiber residues have 2.5 times the cellulose content reported in the literature.

According to Oliveira Júnior *et al.*<sup>27</sup> guaraná fiber has 19.16 ± 1.07% cellulose. In principle, the difference in the amount of cellulose is due to the method used to extract the fibers from the seeds of guaraná. For Yan *et al.*<sup>29</sup> the amount of cellulose present in the fibers directly influences their strength, stiffness and stability.

The XRD patterns (Figure 2b) basically show the main reflections of cellulose from 15° to 25°,<sup>28,30</sup> in addition to the crystallinity percentages of 28.4%, 17.6% and 16.5% for the fibers of açai, guaraná and tucumã, respectively. On the other hand, XRD reflections characterize amorphous phases and with low crystallinity peaks.

The Figures 3a-3c show the surface morphology and fiber distribution of guaraná, tucumã and açai, whose average sizes are 32, 100 and 250 µm, respectively (Figures 3d-f). The average sizes allow for the production of composites with a PP polymer matrix. The morphology of fibers of guaraná is characterized by small fragments with irregular dimensions and contours (Fig 3a, white arrow).<sup>27</sup>

In Figure 3b (green arrow), for the endocarp of tucumã, there is a wide variety of shapes (irregular, rounded and prismatic grains), which is attributed to the milling process.<sup>24</sup> On the other hand, the fiber of açai is characterized by fragments in the form of rods and others of different sizes and shapes (Fig 3c, blue arrow).

Figure 4a shows the TGA curves that correspond to water loss at temperatures close to 100 °C with the following values 16.4, 10.7 and 8.3% for açai, guaraná and tucumã fibers, respectively. The thermograms show typical cellulose, hemicellulose and lignin mass reductions in the range of 270 to 544 °C. The difference in the amount of energy absorbed by the fibers depends on the amount of water they contain and, in this study, they are in accordance with the lignocellulosic analyses that were performed. From 284 °C (Fig. 4b), DSC shows the exothermic transformations until approximately 365 °C corresponding to the decomposition of cellulose, hemicellulose, and lignin as reported in the research of Chand *et al.*<sup>31</sup> These transformations not only coincide but also align perfectly with the wide range of mass reductions observed during thermogravimetric

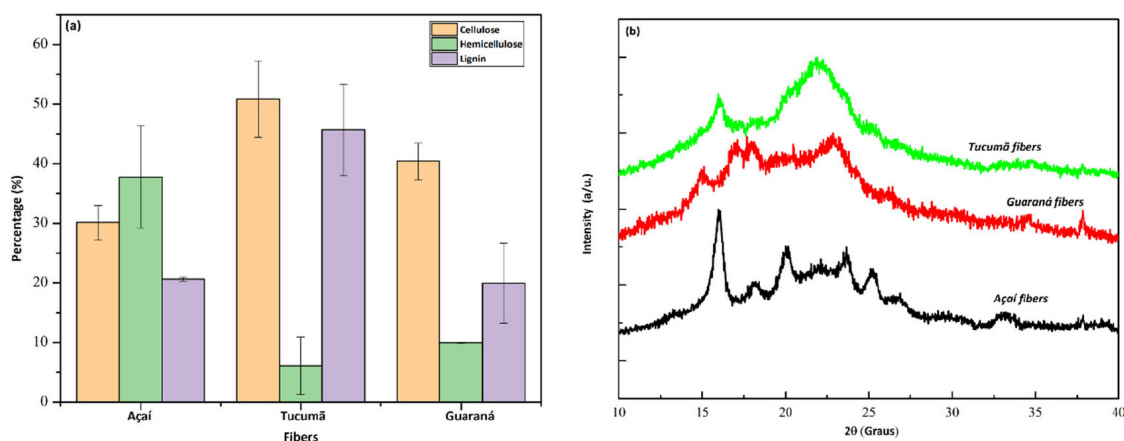
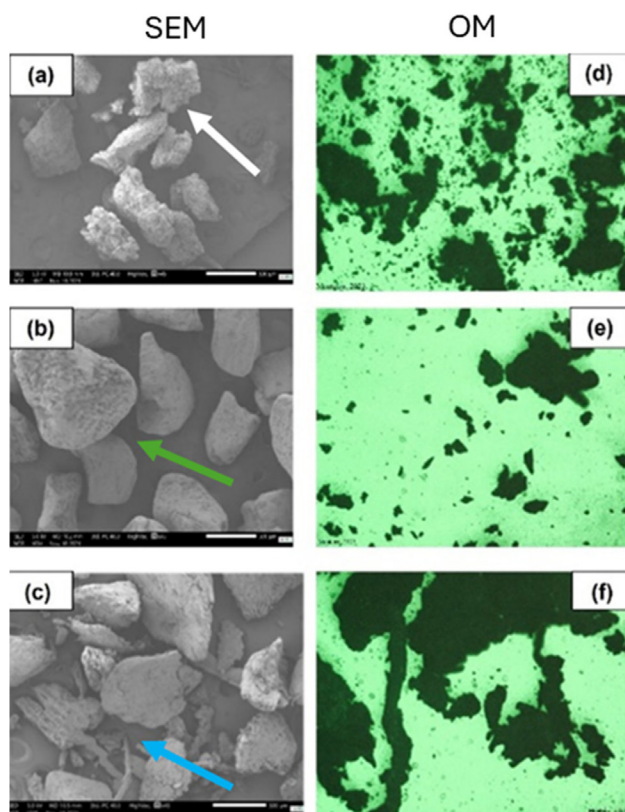


Figure 2. (a) Amount of cellulose, hemicellulose and lignin (b) X-ray diffractograms of fibers of açai, guaraná and tucumã



**Figure 3.** SEM and OM for fibers of (a) and (d) guarana; (b) and (e) tucumã and (c) and (f) açai

analysis (TGA), indicating a significant correlation between the transformation processes and the mass loss recorded throughout the experiment. For açai fibers, DSC shows the exothermic peaks can be visualized at 299.1 and 326.3 °C; 309.90 and 350.4 °C for guaraná fibers; and 284.2 and 364.7 °C for tucumã fibers. Thus, the endothermic and exothermic transformations are in accordance with those visualized in the TGA curves.

Figure 5 presents the FTIR spectra of açai, guaraná, and tucumã fibers, both in their natural state and after heating to 200 °C. The FTIR analysis demonstrates that the fibers maintain thermal stability at 200 °C, which is

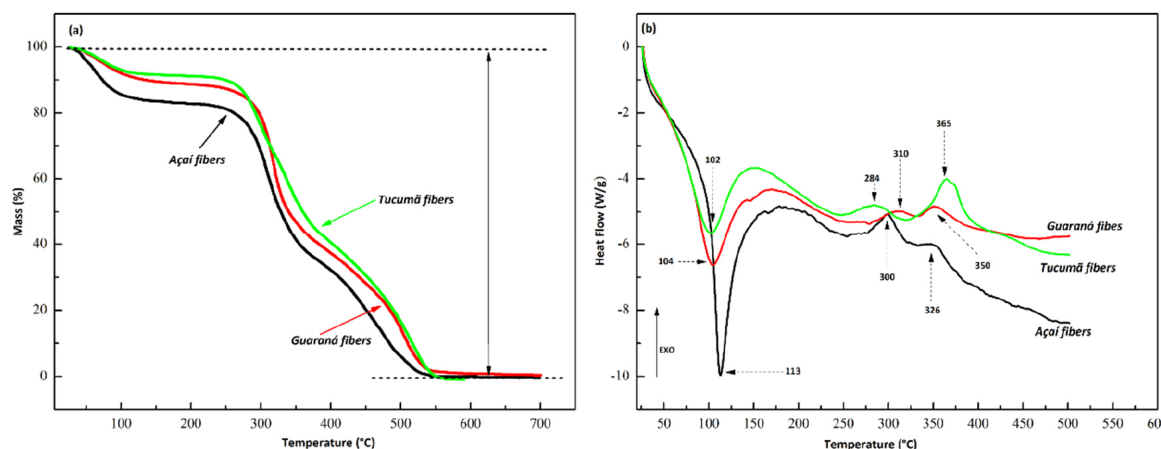


**Figure 4.** Curves of: (a) TGA and (b) DSC for the fibers of açai, guaraná and tucumã

the processing temperature typically required for plastic injection using PP.

In general, the spectra have absorption bands typical of lignocellulosic substances, with functional groups referring to cellulose, hemicellulose and lignin. As such, it is possible to detect absorption bands for the fibers (Figure 5a-c) in the following regions:

- 3336  $\text{cm}^{-1}$ : -OH elongation vibrations arising from hydrogen bonding in cellulose;<sup>14</sup>
- 2912  $\text{cm}^{-1}$ : stretch vibrations characteristic of  $-\text{CH}_2-$  groups of lignocellulosic substances as reported by Stark and Matuana;<sup>32</sup>
- 1645-1625  $\text{cm}^{-1}$ : assigned to the -OH groups of bending mode water molecules adsorbed on the cellulose molecules;<sup>14</sup>
- 1251  $\text{cm}^{-1}$ : C-O stretch vibrations of lignin and hemicellulose as described by Zhang *et al.*;<sup>33</sup>
- 1022  $\text{cm}^{-1}$ : lignin C-O elongation vibration as reported by Kumar *et al.*;<sup>34</sup>
- 664  $\text{cm}^{-1}$ : -COH bending out of the plane of cellulose;<sup>14</sup>

### 3.2. Physical, chemical and thermal properties of biocomposites

The FTIR spectra of the composites basically show absorption bands referring to the fibers of açai, guaraná, tucumã and PP (Figure 6). The spectrum of the PP exhibits typical absorption bands of symmetric deformation of  $\text{CH}_3$  grouping at 1377  $\text{cm}^{-1}$  and stretching of C-H and  $\text{CH}_2$  bonds at 2960 and 2920  $\text{cm}^{-1}$ , respectively.

These bands correspond to those observed in the study by Catto *et al.*<sup>35</sup> on biocomposites of PP and yerba mate (*Ilex paraguariensis*, Saint Hil.) fibers. At 1350  $\text{cm}^{-1}$ , there is an absorption band referring to C-C for PP.<sup>36</sup> In the same way as in the study by Kieling *et al.*<sup>24</sup> in the FTIR of the biocomposites of our study, no absorption bands were observed that might indicate a reaction between the PP and the fibers.

TGA and DSC measurements reveal a small increase in the initial decomposition temperature from PP (297 °C)

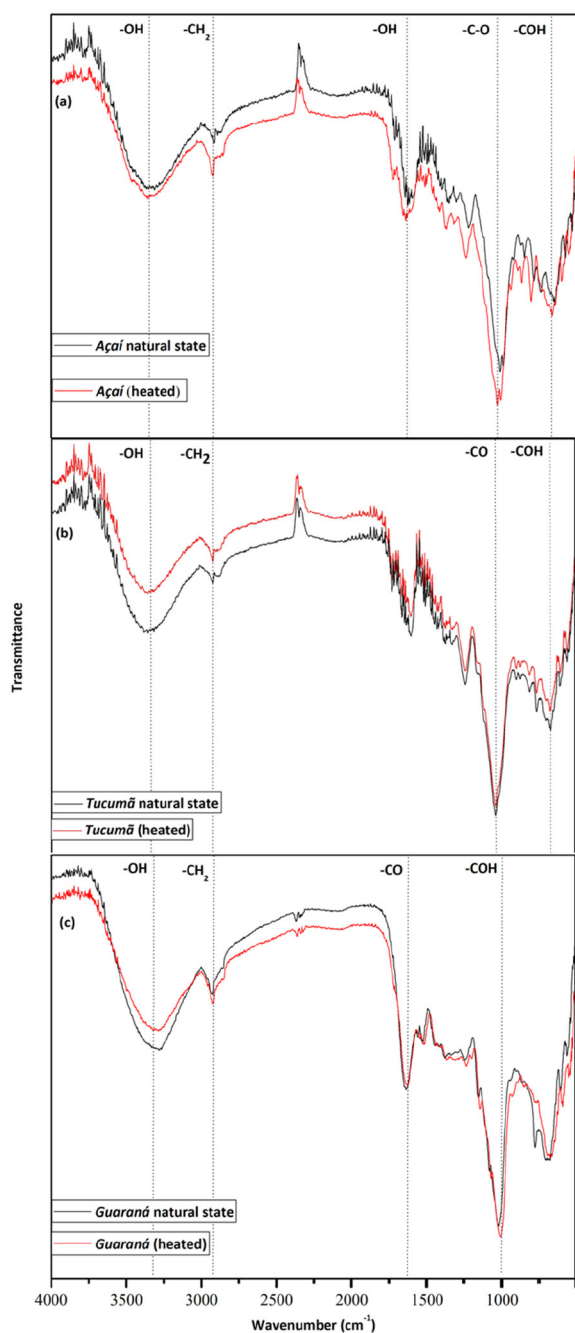


**Figure 5.** FTIR spectrum for the fibers of (a) açai; (b) tucumã and (c) guaraná in their natural state and after heating to 200 °C

to the produced composites ( $300 \pm 0.1$  °C). However, the maximum decomposition temperature varies depending on the composite's composition and the extent of decomposition. For PP, the peak decomposition occurs at 434.5 °C, while for the composites, it is observed at  $457.04 \pm 3.65$  °C. Figure 7a presents the TGA curves for PP and its composites, highlighting their distinct maximum mass loss values: PP:G:T (34.0%); PP:A:T (44.5%); PP:A:G:T (45.5%); PP:A:G (51.6%); PP:A (54.8%); P:G and PP:T (58.0%); and neat PP (46.3%). Furthermore, the final decomposition temperature is 475.1 °C for PP and  $475.3 \pm 0.4$  °C for the composites.

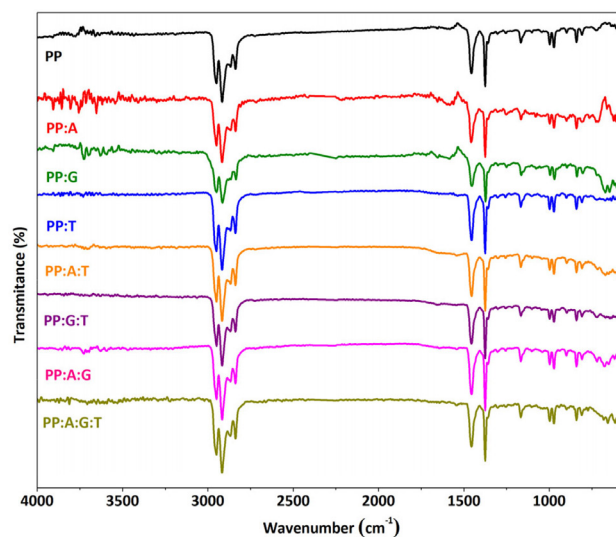


**Figure 6.** FTIR spectra of PP and composites with fibers from açai (A), guaraná (G), tucumã (T)

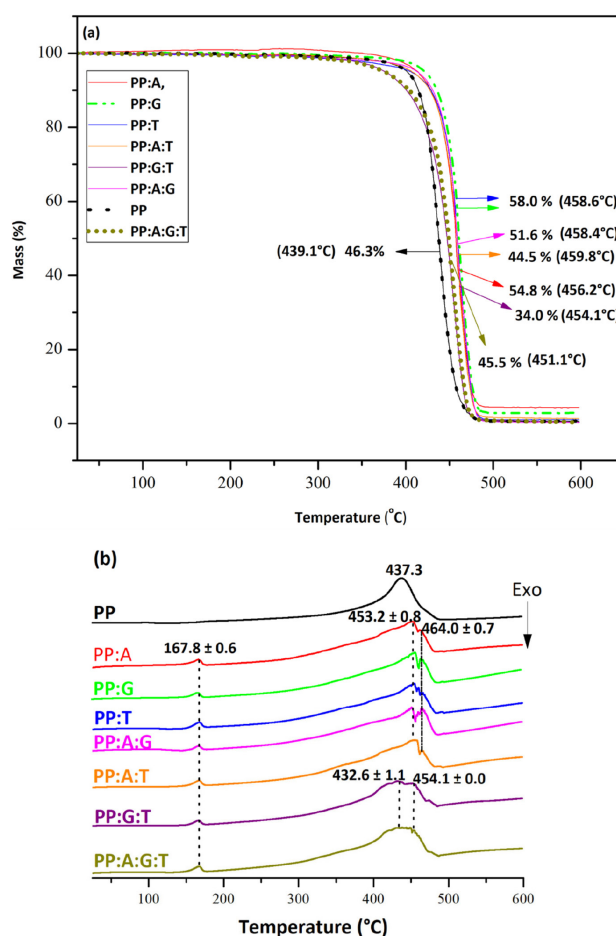


**Figure 7.** Curves of (a) TGA and (b) DSC for PP, PP composites and fibers from açai, guaraná and tucumã

The initial temperature of thermal decomposition ( $T_i$ ) of the PP is 396.8 °C. Decomposition in the range of 269.8 °C to 543.6 °C occurs because of the three main constituents of the natural constituents: cellulose, hemicellulose and lignin (Figure 4a). This behavior is related to the interfacial

interactions between PP and the fibers studied in this work, whose particles can limit the movement of polymer chains, with the breakdown of molecular chains at lower temperatures.<sup>37</sup> The literature states that the thermal decomposition of wood-plastic biocomposites depends on other factors such as the species and the amount of wood, particle size, moisture content, coupling agents, amount and type of polymers and other additives.<sup>38</sup> Thus, the  $T_d$  for a polymer is essential in order to be able to evaluate its thermal stability.<sup>39</sup>

Among the composites, the thermal stability was higher for the PP:A combination followed by similar combinations for (i) PP:G, PP:T and PP:G:T and (ii) PP:A:G, PP:A:T and PP:A:G:T. The processing temperature should be high enough for the polymers to melt and flow but should not exceed the degradation temperature (437.3 °C) to avoid deterioration of their properties. The thermal stability of polymer composites depends on two main factors, *i.e.*, morphology and the interfacial bonding of the mixtures.<sup>40</sup>

In Fig 7b, the DSC curves show endothermic transformations for the PP (437.3 °C) and for the composites (167.8 to 464.0 °C). It is possible to observe a transformation in the region of 437.3 °C that corresponds to the maximum thermal decomposition temperature of PP observed in TGA/DTG curves. For the composites, the transformations occurring in the range from 432.6 to 464.0 °C are compatible with the ranges of mass reductions obtained in TGA, which are characteristic of lignocellulosic components. The transformation at 167.8 °C occurred only for the composites which may be associated with lignin decomposition. This fact was also observed by Yang *et al.*<sup>41</sup> who describe lignin as a substance with a very large decomposition temperature range (160.0 to 900.0 °C); in other words, it is common for the degradation peaks of this substance to be superimposed with other substances.

The micrographs of the fractured cross sections in the tensile are shown in Figure 8a-h. For the PP, an almost predominantly straight rupture can be observed (Figure 8a). According to Kieling *et al.*<sup>24</sup> this type of rupture is common in fragile polymers such as PP, especially pure polymer. For the other composites, it is possible to visualize the displacement of the fibers at rupture (Figure 8b-d) and the morphology according to the study of them individually (Figure 3a-c). Some composites showed microvoids (Figure 8b-d), which according to Kieling *et al.*<sup>24</sup> become evident due to fractures after tensile testing, and the separation between the composite phases is clearly shown.

### 3.3. Mechanical properties of the biocomposites: tensile and flexural tests

The Table 1 shows the test results of tensile mechanical properties. When compared to PP, the biocomposites produced with the addition of 10% of either fibers of tucumã, açai or guaraná (one type of fiber added to PP) had a reduction in tensile strength of about 10.5 to 34.1% and a reduction in modulus of elasticity of 41.13 to 66.41%. On the other hand, the combination of two fibers and PP also reduced the tensile strength by about 16.4 to 36.9% and the modulus of elasticity by 47.25 to 62.64%. Finally, the combination of the three fibers shows an average reduction in strength of 13.3% in relation to the PP matrix and the modulus of elasticity is reduced by 49.76%, obeying the following order FG (guaraná fibers) > FT (tucumã fibers) > FA (açai fibers).

Seixas *et al.*<sup>42</sup> observed a reduction of approximately 20% in the maximum tensile strength for several biocomposites produced with banana stalks and a PP of three different granulometries (32, 48 and 100 mesh). According to these authors, the reduction of maximum tensile strength is

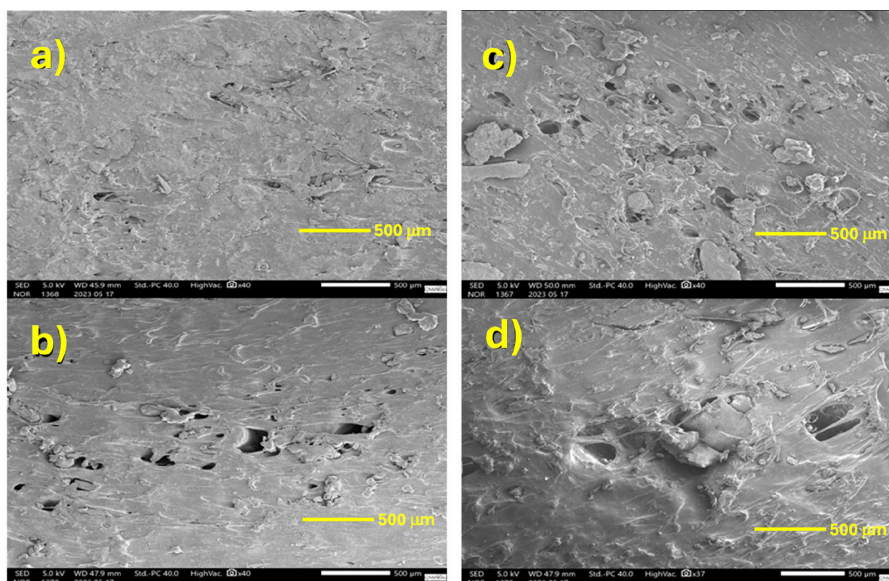


**Figure 8.** Micrographs obtained from the cross sections of the fractures in the tensile test: (a) PP, (b) PP:A, (c) PP:G and (d) PP:T.

directly related to the adhesion process between banana fibers and the PP polymer matrix. Another possibility is the discontinuity effect that prevents a uniform distribution in the polymer matrix that is caused by the fibers.<sup>43</sup> Lopez *et al.*<sup>44</sup> mention that, generally, the effect of short fiber reinforcement on the modulus of elasticity of a thermoplastic matrix is governed by parameters as fiber dispersion and intrinsic fiber stiffness, among others.

Despite the observed changes, these composites stand out as promising materials for engineering applications. The results imply a 10% reduction of PP in the composition of the polymer matrices.

Figure 9 corresponds to the boxplot graphs of the tensile and flexural properties of PP and the respective fiber composites of Amazonian fruits. The boxplots of the composites show that all the proportions used in this study obey a normal distribution. It is possible to observe only one outlier in the boxplot referring to the PP flexural test. In addition, it is observed that for practically all the boxplots there is a small asymmetry, but the data still correspond to a normal distribution.

Another characteristic of the boxplots is the existence of asymmetric whiskers, but still with small differences which does not affect the interpretation of the results. The boxplot of the flexural test shows that there is no significant

difference between PP and all composites. This indicates that the composites have practically the same flexural capacity as PP. However, the same cannot be said in relation to the test of tensile strength and modulus whose medians show significant differences. In other words, the biocomposites produced in this study have an effect on tensile strength. In general terms, the biocomposites produced in this study have a lower tensile capacity than PP.

#### 4. Conclusion

The study of the physical and chemical characteristics of the fibers of açai, guaraná and tucumã showed the following characteristics in their natural state: (i)  $\leq 22.4\%$  moisture; (ii)  $\leq 50.9\%$  cellulose; (iii)  $\leq 37.8\%$  hemicellulose; (iv)  $\leq 45.7\%$  lignin; (v)  $\leq 28.4\%$  crystallinity; and (vi) endo- and exothermic transformations between 269 °C and 544 °C. The fibers studied in this work have particles of different sizes, shapes (irregular granular, rounded, primastic, rod-like and acicular) and regions with porosities. The physicochemical analyses of the biocomposites did not reveal the formation of new crystalline phases during the plastic injection.

Nonetheless, the start of the degradation of PP

**Table 1.** Tensile and flexural properties of PP and the composites reinforced with vegetable fibers from the Amazon

Samples	Tensile		Flexural	
	Resistance (MPa)	Module (GPa)	Resistance (MPa)	Module (GPa)
PP	17.11±1.65	1.27±0.10	26.33±0.95	0.87±0.04
PP:G	15.32±0.96	0.75±0.04	28.03±0.56	0.87±0.03
PP:T	13.06±0.21	0.67±0.01	26.65±0.80	0.89±0.04
PP:A	11.28±0.76	0.43±0.02	21.63±1.70	0.71±0.07
PP:A:G	14.31±0.46	0.63±0.02	27.46±0.65	0.87±0.07
PP:G:T	11.18±0.20	0.45±0.01	22.96±1.33	0.78±0.03
PP:A:T	10.80±1.83	0.48±0.03	20.54±0.87	0.65±0.05
PP:A:G:T	14.84±0.40	0.64±0.01	26.72±0.47	0.89±0.02

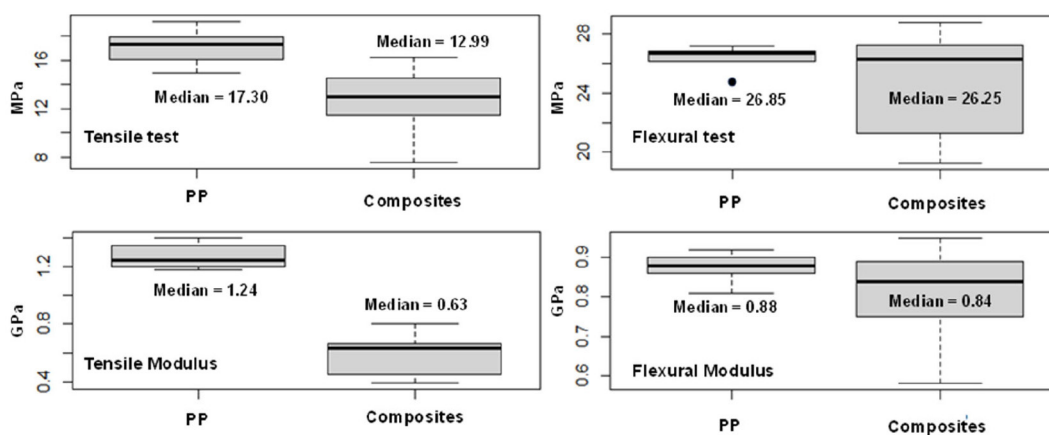


**Figure 9.** Boxplot of tensile test, tensile modulus, flexural test and flexural modulus of açai, guaraná and tucumã fiber-reinforced composites

occurs at 396.8 °C and ends at 475.1 °C, while in the biocomposites the temperature is reduced to 300 °C, but the end is maintained at about 475 °C. Another difference is the endothermic transformations, which in PP occurs at 437.3 °C and in the composites from 167.8 to 464.0 °C. The rupture of biocomposites occurred with the formation of microvoids that are typical of conglomerates with distinct phases. Despite this, the biocomposites produced in this study have a lower tensile strength than PP.

## Acknowledgments

The authors would like to thank the Analytical Center of the Federal Institute of Education, Science and Technology of Amazonas (IFAM - *Campus* Manaus city center), Tutiplast Company, Magama Industrial, Amazon Biotechnology Center (CBA), Multi-user Center for Analysis in Biomedical Phenomena (CMABIO) at the Amazonas State University (UEA), Laboratory of Synthesis and Characterization of Nanomaterials (LSCN) at IFAM - *Campus* Industrial District, Laboratory of Natural Products and Electrochemistry/Energy at the Federal University of Amazonas (UFAM) and the Higher School of Technology at UEA. Authors also thank to Coordenação de Aperfeiçoamento de Pessoal de Nível Superior - Brasil (CAPES) - Finance Code 001.

## Bibliographic References

- Silva, R. S.; Santos, C. L.; Mar, J. M.; Kluczkowski, A. M.; Figueiredo, J. A.; Borges, S. V.; Bakry, A. M.; Sanches, E. A.; Campelo, P. H.; Physicochemical properties of tucumã (*Astrocaryum aculeatum*) powders with different carbohydrate biopolymers. *LWT-Food Science and Technology* **2018**, *94*, 79. [Crossref]
- Instituto Nacional de Pesquisas Espaciais (INPE); Monitoramento do desmatamento da floresta Amazônica brasileira por satélite; Available in: <<http://www.obt.inpe.br/OBT/assuntos/programas/amazonia/prodes>>. Access in: December 21<sup>th</sup>, 2024.
- Homma, A. K. O.; *Extrativismo, Biodiversidade e Biopirataria na Amazônia*, Embrapa Informação Tecnológica: Brasília, 2008.
- Ferreira, J. C. B.; Silva-Cardoso, I. M. A.; Meira, R. O.; Scherwinski-Pereira, J. E.; Somatic embryogenesis and plant regeneration from zygotic embryos of the palm tree *Euterpe precatoria* Mart. *Plant Cell Tissue and Organ Culture* **2022**, *148*, 667. [Crossref]
- Schulz, M.; Borges, G. da S. C.; Gonzaga, L. V.; Costa, A. C. O.; Fett, R.; Juçara fruit (*Euterpe edulis* Mart.): Sustainable exploitation of a source of bioactive compounds. *Food Research International* **2016**, *89*, 14. [Crossref]
- Rocha, E.; Potencial ecológico para o manejo de frutos de açazeiro (*Euterpe precatoria* Mart.) em áreas extrativistas no Acre, Brasil. *Acta Amazônica* **2004**, *34*, 237. [Crossref]
- Barbosa, J. R.; Junior, R. N. C.; Food sustainability trends - How to value the açai production chain for the development of food inputs from its main bioactive ingredients? *Trends Food Science Technology* **2022**, *124*, 86. [Crossref]
- Pacheco-Palencia, L. A.; Duncan, C. E.; Talcott, S. T.; Phytochemical composition and thermal stability of two commercial açai species, *Euterpe oleracea* and *Euterpe precatoria*. *Food Chemistry* **2009**, *115*, 1199. [Crossref]
- Instituto Brasileiro de Geografia e Estatística (IBGE); *Quantidade produzida de açai, em toneladas, em lavouras permanentes*; IBGE 2022. Available in: <<https://sidra.ibge.gov.br/tabela/1613#resultado>>. Access in: December 9<sup>th</sup>, 2024.
- S. A. Vianna.; *Astrocaryum aculeatum* G. Mey. Available in: <<https://floradobrasil2020.jbrj.gov.br/FB22080>>. Access in: December 11<sup>th</sup>, 2024.
- Kieling, A. C.; Santana, G. P.; dos Santos, M. C.; Jaqtinon, H. de C. C.; Monteiro, C. C. P.; Cadeia do tucumã comercializado em Manaus-AM. *Scientia Amazônia* **2019**, *8*, 2019. [Link]
- Somner, G. V.; Medeiros, H.; *Paullinia cupana*. Available in: <<https://monografiasfloradobrasil.jbrj.gov.br/paullinia.pdf>>. Access in: December 11<sup>th</sup>, 2024.
- Da Silva Junior A. L. S.; Nascimento, M. M.; Santos, A. G.; Lôbo, I. P.; de Jesus, R. M.; Occurrence of polycyclic aromatic compounds in guarana (*Paullinia cupana*) seeds subjected to different drying processes. *Applied Food Research* **2022**, *2*, 100110. [Crossref]
- Rocha, M. I.; Benkendorf, S.; Gern, R. M. M.; Riani, J. C.; Wisbeck, E.; Desenvolvimento de biocompósitos fúngicos utilizando resíduos industriais. *Revista Matéria* **2020**, *25*, 1. [Crossref]
- Khalid, M. Y.; Rashid, A. A.; Arif, Z. U.; Ahmed, W.; Arshad, H.; Zaidi, A. A.; Natural fiber reinforced composites: Sustainable materials for emerging applications. *Results in Engineering* **2021**, *11*, 100263. [Crossref]
- Albinate, S. R.; Pacheco, E. B. A. V.; Visconte, L. L. Y.; Revisão dos tratamentos químicos da fibra natural para mistura com poliolefinas. *Química Nova* **2013**, *36*, 114. [Crossref]
- Sasmal, S.; Goud, V. V.; Mohanty, K.; Characterization of biomasses available in the region of North-East India for production of biofuels. *Biomass and Bioenergy* **2012**, *45*, 212. [Crossref]
- Sathishkumar, T. P.; Navaneethkrishnan, P.; Shankar, S.; Rajasekar, R.; Rajini, N.; Characterization of natural fiber and composites - A review. *Journal of Reinforced Plastics and Composites* **2013**, *32*, 1457. [Crossref]
- de Souza, W. B.; Santan, G. P.; de Oliveira, D. L.; Kieling, A. C.; del Pino, G. C.; Júnior, S. D.; Neto, J. C. M.; Composite Materials Using Mallow Fiber and Epoxy Resin. *Revista Virtual de Química* **2024**, *16*, 296. [Crossref]
- Madhu, P.; Sanjay, M. R.; Jawaid, M.; Siengchin, S.; Khan, A.; Pruncu, C. I.; A new study on effect of various chemical treatments on Agave Americana fiber for composite reinforcement: Physico-chemical, thermal, mechanical and morphological properties. *Polymer Testing* **2020**, *85*, 106437. [Crossref]
- Rahman, M. Z.; Xu, H.; Damping under Varying Frequencies, Mechanical Properties, and Failure Modes of Flax/Polypropylene Composites. *Polymers* **2023**, *15*, 1042. [Crossref]

22. Sanjay, M. R.; Madhu, P.; Jawaid, M.; Senthamaraiannan, P.; Senthil, S.; Pradeep, S.; Characterization and properties of natural fiber polymer composites: A comprehensive review. *Journal of Cleaner Production* **2018**, *172*, 566. [[Crossref](#)]
23. Sampaio, M. B.; Carrazza, L. R.; Em *Manual tecnológico de aproveitamento integral do fruto e da folha do Buriti (Mauritia flexuosa)*; De Almeida, F. V. R.; Araújo, R.; Instituto Sociedade, População e Natureza (ISPN): Brasília, 2012.
24. Kieling, A. C.; Santana, G. P.; dos Santos, M. C.; Neto, J. C. de M.; Del Pino, G. G.; dos Santos, M. D.; Duvoisin, S. J.; Panzera, T. H.; Wood-plastic Composite Based on Recycled Polypropylene and Amazonian Tucumã (*Astrocaryum aculeatum*) Endocarp Waste. *Fibers and Polymers* **2021**, *22*, 2834. [[Crossref](#)]
25. Morais, J. P. S.; Rosa, M. de F.; Marconcini, J. M.; Em *Procedimentos para análise lignocelulósica*; Embrapa Algodão: Campina Grande, 2010.
26. Sobreira, T. G. P.; da Silva, L. A.; de Menezes, F. D.; França, E. J.; Aquino, K. A. da S.; Aspectos estruturais de esferas de quitosana/PVA reticuladas com glutaraldeído submetidas a diferentes tratamentos térmicos. *Química Nova* **2020**, *43*, 1251. [[Crossref](#)]
27. de Oliveira Júnior, S. D.; Gouvêa, P. R. dos S.; de Aguiar, L. V. B.; Pessoa, V. A.; Costa, C. L. dos S. C.; Chevreuil, L. R.; Production of Lignocellulolytic Enzymes and Phenolic Compounds by *Lentinus strigosus* from the Amazon Using Solid-State Fermentation (SSF) of Guarana (*Paullinia cupana*) Residue. *Applied Biochemistry and Biotechnology* **2022**, *194*, 2882. [[Crossref](#)]
28. Barros, S. de S.; Oliveira, E. da S.; Pessoa Jr, W. A. G.; Rosas, A. L. G.; de Freitas, A. E. M.; Lira, M. S. de F.; Calderaro, F. L.; Saron, C.; de Freitas, F. A.; Waste açafá (Euterpe precatoria Mart.) seeds as a new alternative source of cellulose: Extraction and characterization. *Research, Society and Development* **2021**, *10*, 1. [[Crossref](#)]
29. Yan, L.; Kasal, B.; Huang, L.; A review of recent research on the use of cellulosic fibres, their fibre fabric reinforced cementitious, geo-polymer and polymer composites in civil engineering. *Composites Part B: Engineering* **2016**, *92*, 94. [[Crossref](#)]
30. Mayakun, J.; Klinkosum, P.; Chaichanasongkram, T.; Kaewtatip, S. S.; Characterization of a new natural cellulose fiber from Enhalus acoroides and its potential application. *Industrial Crops and Products* **2022**, *186*, 115285. [[Crossref](#)]
31. Chand, N.; Sood, S.; Singh, D. K.; Rohatgi, P. K.; Structural and thermal studies on sisal fibre. *Journal of Thermal Analysis* **1987**, *32*, 595. [[Crossref](#)]
32. Stark, N. M.; Matuana, L. M.; Characterization of weathered wood-plastic composite surfaces using FTIR spectroscopy, contact angle, and XPS. *Polymer Degradation and Stability* **2007**, *92*, 1883. [[Crossref](#)]
33. Zhang, P.; Dong, S.-J.; Ma, H.-H.; Zhang, B.-X.; Wang, Y.-F.; Hu, X.-M.; Fractionation of corn stover into cellulose, hemicellulose and lignin using a series of ionic liquids. *Industrial Crops and Products* **2015**, *76*, 688. [[Crossref](#)]
34. Kumar, R.; Sivaganesan, S.; Senthamaraiannan, P.; Saravanakumar, S. S.; Khan, A.; Daniel, S.; Loganathan, L.; Characterization of New Cellulosic Fiber from the Bark of *Acacia nilotica* L. Plant. *Journal of Natural Fibers* **2022**, *19*, 199. [[Crossref](#)]
35. Catto, A. L.; Junior, M. A. D.; Hansen, B.; Francisquetti, E. L.; Borsoi, C.; Characterization of polypropylene composites using yerba mate fibers as reinforcing filler. *Composites Part B: Engineering* **2019**, *174*, 106935. [[Crossref](#)]
36. Cabra, J. R.V.; Identificación de polímeros por espectroscopía infrarroja. *Revista Ontare* **2017**, *5*, 115. [[Crossref](#)]
37. Kumar, D.; Srisvatan, A.; Gautam, V.; Investigation on mechanical and thermo-mechanical properties of injection molded PP-TiO<sub>2</sub> composites. *Materials Today: Proceeding* **2021**, *44*, 4607. [[Crossref](#)]
38. Jeskea, H.; Schirpb A.; Cornelius, F.; Development of a thermogravimetric analysis (TGA) method for quantitative analysis of wood flour and polypropylene in wood plastic composites (WPC). *Thermochimica Acta* **2012**, *543*, 165. [[Crossref](#)]
39. Abdelwahab, M. A.; Flynn, A.; Chiou, B.-S.; Imam, S.; Orts, W.; Chiellini, E.; Thermal, mechanical and morphological characterization of plasticized PLA-PHB blends. *Polymer Degradation and Stability* **2012**, *97*, 1822. [[Crossref](#)]
40. Shayuti, M. S. M.; Sharudin, R. W.; Mohd, T. A. T.; Khamaruddin, P. N. F. M.; Abdullah, M. Z.; Yusoff, P. S. M. M.; Thermal Conductivity and Crystallography of Polypropylene/ Polycarbonate/ Polypropylene-Graft-Maleic Anhydride Polymer Blend. *Materials Science Forum* **2020**, *995*, 56. [[Crossref](#)]
41. Yang, H.; Yan, R.; Chen, H.; Lee, D. H.; Zheng, C.; Characteristics of hemicellulose, cellulose and lignin pyrolysis. *Fuel* **2007**, *86*, 1781. [[Crossref](#)]
42. Seixas, J. N.; Granada, J. E.; Melo, C. C. N.; Silva, G. E. H.; Passador, F. R.; Cholant, G. M.; Oliveira, A. D.; Beatrice, C. A. G.; Gonçalves, M. R. F.; Carreño, N. N. L. V.; Compósitos poliméricos reforçados com fibras naturais do talo da bananeira utilizando diferentes variações de granulometria. *Revista Brasileira de Engenharia e Sustentabilidade* **2018**, *5*, 32. [[Link](#)].
43. Padilha Jr, E. J.; Zard, C. L.; Comportamento mecânico e reológico de compósitos de polipropileno e fibras de bananeira: influência do teor de fibra. *Revista Eletrônica de Materiais e Processo* **2010**, *5*, 10. [[Link](#)]
44. Lopez, J. P.; Mutjé, P.; Peláech, M. A.; Mansouri, N.-E. E.; Boufi, Vilaseca, S.; F.; Analysis of the tensile modulus of polypropylene composites reinforced with stone groundwood fibers. *Bioresources* **2012**, *7*, 1310. [[Crossref](#)]